7.1 STABILITY AND EVOLUTION OF DENSE CURRENTS ON SLOPING TOPOGRAPHY

B. R. Sutherland* , J. Nault, K. Yewchuk and G. E. Swaters
University of Alberta, Edmonton, Canada

1. INTRODUCTION

Driven by a need to understand the propagation and stability of abyssal ocean currents, there have been numerous idealised studies examining the dynamics in a rotating frame of reference of dense fluid on a slope underlying a less dense ambient fluid. This circumstance is characteristic, for example, of the Denmark Strait Overflow and the Western Boundary Undercurrent. A starting point of many theoretical and numerical studies has been to assume the ambient is stationary and the current moves initially at a constant speed set by geostrophic balance. However, recent laboratory experiments (e.g. Lane-Serff and Baines (1998)) have shown that the continuous injection of a dense current from a localised source can significantly accelerate the ambient fluid and the consequent interaction between the two moving fluids cannot be neglected.

We have performed a series of laboratory experiments designed to examine the temporal as well as spatial stability characteristics of an axisymmetric current on a sloping bottom with an overlying non-stationary ambient (Sutherland *et al.* (2003a; 2003b)).

2. EXPERIMENTAL SET-UP

The experiments were performed on a 1 metre diameter rotating table. A 2 metre tall superstructure is fastened to the table to which cameras, lighting, and a fluid reservoir are mounted. A cylindrical acrylic tank with an inner diameter of 90.7 cm and a height of 30.0 cm was centred on the table. Conical-shaped bottom topography was fixed to the bottom of the tank. The cone had height $H_c = 3.0\,\mathrm{cm}$ and radius $R_T = 45.0\,\mathrm{cm}$, as shown in Figure 1.

An annulus of width $W_0 = 0.9\,\mathrm{cm}$ and mean radius $R_0 = 15.0\,\mathrm{cm}$ encircled the cone. It was through this annulus that fluid was injected during the course of an experiment to create a gravity current on a sloping bottom.

With the apparatus in place, the tank was filled to depth H_T with fresh water of density ρ_0. A reservoir containing a dyed salt-water solution was stationed at a height of 2 m above the bottom of the tank. When a valve was opened, this fluid was injected into the center of the cone and ultimately upwards through the annulus.

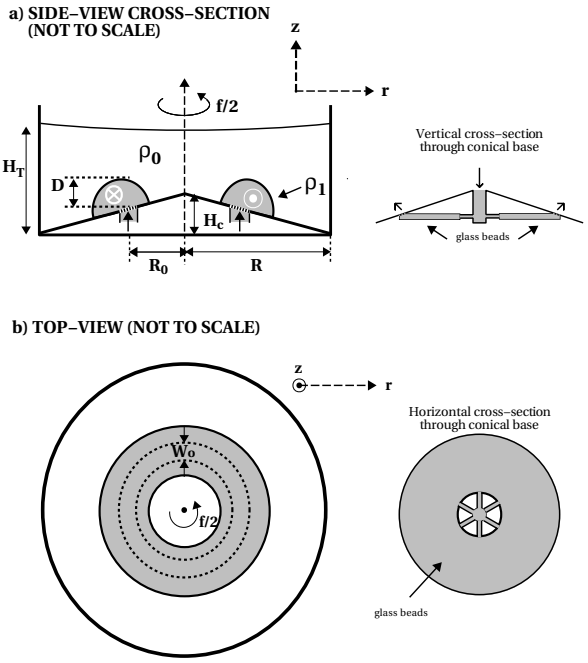

FIG. 1. a) Side view and b) top view schematics of tank and apparatus used to introduce an axisymmetric dense current in a rotating ambient fluid. Relevant dimensional parameters are also illustrated.

There were four parameters that we adjusted in a range of experiments. These were the rotation rate of the table, Ω, the initial depth of the fresh water in the tank before it rotates, H_T, the density of the fluid in the reservoir, ρ_1, and the injection time T_{inj}.

So that large surface deflections and fast downslope motions are avoided, most of our analyses are is performed for experiments with $\Omega \leq 1.0$ and $\sigma \equiv 1000(\rho_1 - \rho_0)/\rho_0 = 0.7$.

A digital still-camera was used to take snapshots of the experiment from the side and from a top perspective angle. A grid of horizontal lines on one side of the tank was used to identify vertical distances

*Corresponding author: Dept. Mathematical and Statistical Sciences, U. Alberta, Edmonton, AB T6G 2G1, Canada;
e-mail: bruce.sutherland@ualberta.ca;
web: http://taylor.math.ualberta.ca/~bruce

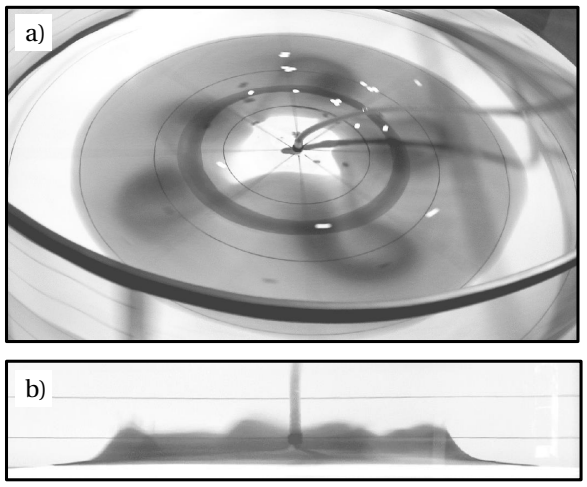

FIG. 2. a) Perspective view and b) side view of an experiment in which the dyed dense current becomes unstable. The experimental parameters are $\Omega = 1.0\,\mathrm{s}^{-1}$, $\mathrm{H_T} = 15\,\mathrm{cm}$, $\sigma = 1.07$ and $\mathrm{T_{inj}} = 30\,\mathrm{s}$. The horizontal lines in b) are spaced vertically by 5cm. The horizontal extent of the image in b) has been magnified with respect to that in a).

and so measurements of the height of the dyed current could be made from the side view snapshots. For example, Figure 2 shows snapshots taken in a typical experiment in which the dense current becomes unstable to 5 wavelengths around the annulus.

As well as the still-camera images, the experiments were recorded continuously in the co-rotating frame by a COHU CCD camera mounted 2m above the table. These images were digitized and analyzed using the software "DigImage" ((Dalziel 1993)). Surface tracers were used to record the surface flow speed. In experiments in which the current became unstable, the wavelength and phase speed of the instability were also measured.

3. QUALITATIVE OBSERVATIONS

In successful experiments, the fluid emerged approximately uniformly around the annulus and assumed a dome-shaped axisymmetric structure. Coincident with the building up the current is the development of an Ekman layer. This is apparent, for example, in Fig. 2b as the thin (approximately 1mm deep) tongue of dyed fluid moving radially in advance of the domed current.

As soon as the fluid injection begins, an axisymmetric current develops in the overlying ambient fluid. This is visualised by the motion of passive tracers on the surface.

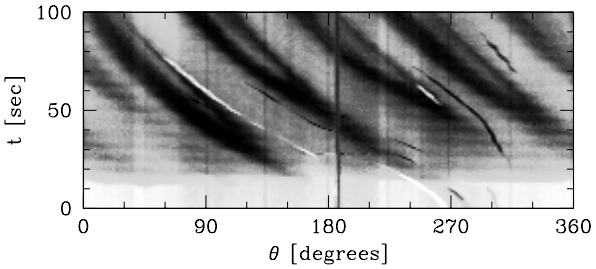

FIG. 3. Time series determined around a circle of radius 18cm. Θ increases in a counter-clockwise direction around the ring. Experimental parameters are the same as those given in the caption of Fig. 2.

The dynamics of the current and surface flow are neatly summarised by circular time series images such as the one shown in Figure 3. The time series is constructed by recording over time the evolution of the flow around a ring of radius $R_{TS} = 18\,\mathrm{cm}$, moderately wider than the mean radius of the annulus.

Soon after the injection begins, the Ekman layer reaches this ring. This is apparent from the uniform darkening of intensities around it. A short time later, a periodic pattern of even darker intensity regions appears. These reflect the unstable undulations in the dense current at $r = 18\,\mathrm{cm}$, and their slope in the space-time plot gives the speed of propagation of the instability. The negative slope indicates the instability progresses in a clockwise direction, opposite to the direction of rotation of the table: the instability is anticyclonic.

Also apparent in Fig 3 are white streaks, which are formed by the approximately circular motion of the surface tracer particles. The streaks form lines with the same slope as the underlying dark intensity regions. Thus the surface flow and, presumably, the whole vertical column of the ambient fluid moves at the same speed as the instability. In general, very little motion is observed for particles between the center of the tank and the inside edge of the annulus, whereas the particles on the outside edge of the annulus move substantially as soon as dense fluid is injected.

This observation indicates a significant difference between the initial conditions of the experiments and those imposed in the theories of Swaters (1991) and Griffiths *et al.* (1982) who assumed an initially stationary ambient layer overlying a geostrophically balanced current. In the experiments not only is the ambient flow non-stationary, but the equal surface flow speeds and unstable mode phase speeds indicates that the ambient region significant affects the

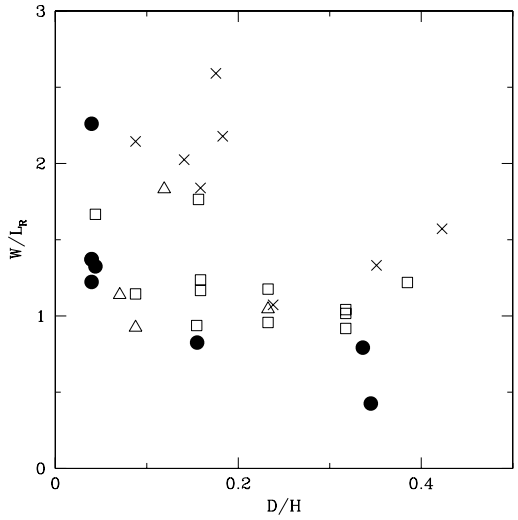

FIG. 4. Regime diagram showing stability of current as a function of nondimensional current width and depth. Solid circles indicate experiments in which the current remains stable. Other symbols are drawn for experiments in which the flow becomes unstable to a mode with wavenumber 4 (open triangles), wavenumber 5 (open squares) and wavenumber 6 (crosses).

instability dynamics.

4. QUANTITATIVE ANALYSIS

The stability regimes are indicated in Fig. 4, which illustrates whether instability occurs as a function of the depth D and width W of the current. Both axes are made nondimensional by the total fluid depth H and the Rossby radius $L_R = (g'\bar{h})^{1/2}$, respectively. Here $\bar{h} = [D(H-D)]^{1/2}$. In general we find the current is stable (as indicated by the solid circles) if either of W/L_R or D/H is small.

In experiments in which instability occurs typically the current breaks into unstable modes with wavenumbers, N_λ, typically between 4 and 6, as indicated by the different symbols in Fig. 4.

We compare the wavenumber and phase speed of the observed modes with those predicted by Choboter and Swaters (2000), examining in particular how the number of waves of instability and the relative phase speed varies with the "Swaters interaction parameter" $\mu = D/(H\tilde{s})$. This is a measure of the destabilizing effect of baroclinicity relative to the stabilizing effect of the beta-plane slope. In their theory, μ must be of order unity. Nonetheless they extrapolate their results to large μ.

Assuming a stationary upper layer, Choboter and Swaters (2000) predict that the flow is unstable for all μ and that N_λ increases with μ. For example, they find N_λ increases from 5 to 15 as μ increases from 1 to 10. As shown in Figure 5a, we find that the observed wavenumber does not vary significantly with μ. Possibly there exists a weakly increasing trend, but the data are too scattered to draw any definitive conclusions.

The phase speed predicted by Choboter and Swaters (2000) also differs. They predict that the ratio of the phase speed to Nof speed, $C_{\mathrm{Nof}} = g's/f$, should be approximately unity for a wide range of interaction parameters. However, as shown in Figure 5b, we find that the phase speed is an order of magnitude smaller than the Nof velocity for small μ. For large μ the relative phase speed varies between 0.1 and 1.

The reason for the discrepancy is that, at least in experiments with small σ, the evolution of the current is governed not by the baroclinic dynamics of the current but by the barotropic dynamics of the surface flow.

A crude theory allows us to estimate the characteristic azimuthal (linear) speed, C_0, of the surface flow. Ignoring the beta-plane dynamics induced by the slope, we compute the initial potential vorticity of the fluid directly over the annulus to be $Q_0 = f/H$. Now suppose the injected fluid compresses the upper layer to a depth of $H - D$. For conservation of potential vorticity, anticyclonic vorticity, $\zeta < 0$, must develop in the upper layer. Using the shallow water expression for potential vorticity, $Q = (f+\zeta)/(H-D)$, its conservation requires

$$\zeta = -\frac{fD}{H} \tag{1}$$

Because this region of induced vorticity forms a current around a circle of radius R_0, we write $\zeta = 2(2\pi/T)$ where the period $T = 2\pi R_0/C_0$. Thus

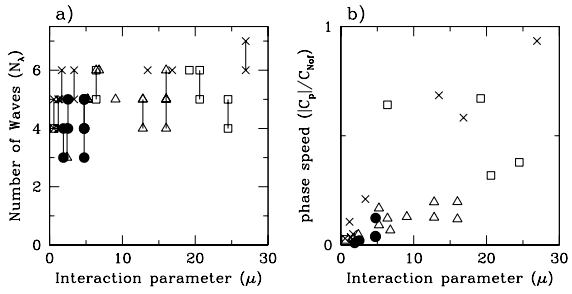

FIG. 5. a) Number of waves of instability and b) nondimensional phase speed both plotted as functions of the interaction parameter μ, which measures the relative importance of baroclinicity for destabilization of the current.

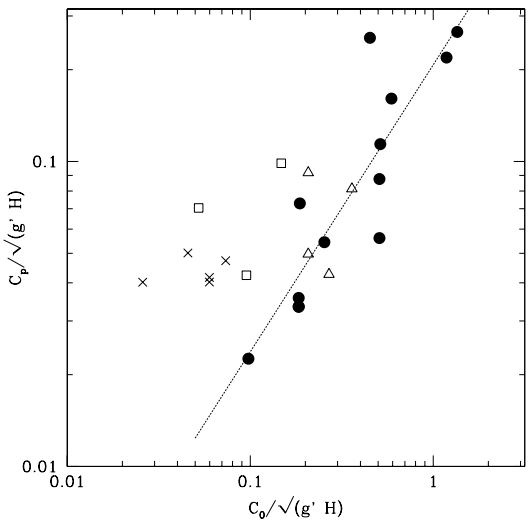

FIG. 6. Phase speed of the unstable modes versus estimated upper-layer speed determined from PV conservation arguments. Different symbols are plotted depending on the relative density of the injected fluid: solid circles for $\sigma \leq 8$, open triangles for $8 < \sigma \leq 16$, open squares for $16 < \sigma \leq 64$, and crosses for $\sigma > 64$. The dotted line represents the best fit line through data with $\sigma < 8$ (solid circles).

we predict

$$C_0 = -\frac{\Omega D R_0}{H}. \qquad (2)$$

If the instability of the lower current is indeed controlled by barotropic instability of the surface flow, we expect that C_p should be proportional to C_0. In Figure 6 we plot C_p versus C_0, with both axes normalized by the shallow water speed based on the total fluid depth H.

For relatively low density currents, plotted with solid circles in the figure, the phase speed clearly increases with C_0. Indeed, a best fit line through these points gives a slope of 0.94 ± 0.08, which is consistent with the expected slope of 1. For currents with large densities, $\sigma > 64$, the phase speed is found to be approximately constant.

A transition to new, presumably baroclinic, dynamics occurs for $\sigma \gtrsim 16$. These are captured neither by eq. (2) nor by existing baroclinic theories that neglect the induced motion of the ambient fluid (*e.g.* Swaters (1991)).

5. CONCLUSIONS

We have constructed a novel experimental apparatus that allows us to examine bottom-dwelling dense axisymmetric currents without explicitly disturbing the surface as one would, for example, by rapidly extracting two concentric cylinders in a standard lock-release mechanism.

Instability is observed in experiments with bottom flows that are sufficiently deep compared with the total fluid depth and sufficiently wide compared with the Rossby radius L_R. If the density of the bottom current is relatively small, the observed instability of the current is driven entirely by barotropic instability of the surface jet in a manner that can be understood by potential vorticity conservation arguments.

For currents that are more dense ($\sigma \gtrsim 16$), no theory presently exists that predicts the unstable characteristics of a dense current with a overlying non-stationary ambient. In ongoing research we will develop a better understanding of this system through analysis of numerical simulations that model the bottom injection of fluid.

References

Choboter, P. and Swaters, G. E. 2000. On the baroclinic instability of axisymmetric rotating gravity currents with bottom slope. *J. Fluid Mech.*, 408:149–177.

Dalziel, S. B. 1993. Rayleigh-Taylor instability: experiments with image analysis. *Dyn. Atmos. Oceans*, 20:127–153.

Griffiths, R. W., Killworth, P. D., and Stern, M. E. 1982. Ageostrophic instability of ocean currents. *J. Fluid Mech.*, 117:343–377.

Lane-Serff, G. F. and Baines, P. G. 1998. Eddy formation by dense flows on slopes in a rotating fluid. *J. Fluid Mech.*, 363:229–252.

Sutherland, B. R., Nault, J., Yewchuk, K., and Swaters, G. E. 2003a. Rotating dense currents on a slope. Part I: Stability. *J. Fluid Mech.*, in preparation.

Sutherland, B. R., Yewchuk, K., Nault, J., and Swaters, G. E. 2003b. Rotating dense currents on a slope. Part II: Nonlinear evolution. *J. Fluid Mech.*, in preparation.

Swaters, G. E. 1991. On the baroclinic instability of cold-core coupled density fronts on a sloping continental shelf. *J. Fluid Mech.*, 224:361–382.